Synthesis, Structure, and Dynamic Behavior of *ansa*-Ferrocenes with Pyrazabole Bridges†

Frieder Jäkle, Thomas Priermeier, and Matthias Wagner*,‡

Anorganisch-chemisches Institut der Technischen Universität München, Lichtenbergstrasse 4, D-85747 Garching, Germany

Received December 4, 1995⊗

A variety of stereorigid *ansa*-ferrocenes **2** with *o*-phenylene-type bridges have been obtained by the reaction of 1,1′-diborylferrocenes (1,1′-Fc(BBrR)$_2$; Fc = ferrocenyl; R = CH_3, Br, OEt, NC_4H_8) with selected pyrazole derivatives. Subsequent intramolecular B−N adduct formation establishes the interannular bridges. The synthetic approach is based on the replacement of certain critical carbon−carbon links by the isoelectronic, self-assembling, dative boron−nitrogen bonds and thus follows the principles of noncovalent synthesis. The pyrazabole bridge does not seem to cause any significant distortion of the ferrocene core. Most substituents at boron or pyrazole lead to an *ansa*-ferrocene structure. However, the presence of both strong electron donors (i.e. pyrrolidine) at boron and strongly electron-withdrawing pyrazole substituents (i.e. ester groups) results in an open chain structure **2i** with three-coordinate boron atoms. The tetravalent boron centers in *ansa*-1,1′-Fc[B(Br)(μ-pz)]$_2$, **2a**, show an unusually high tendency to undergo nucleophilic substitution reactions, even though they are located at bridgehead positions. NMR spectroscopy, as well as chemical evidence argue against an unbridged open chain intermediate in the course of these reactions.

Introduction

ansa-Metallocenes play a prominent role in organometallic chemistry.[1] The introduction of a bridge spanning both Cp rings prevents internal cyclopentadienyl rotation and increases the rigidity of the molecule, which has been exploited, for example, in homogeneous Ziegler−Natta catalysis.[2,3] Furthermore, *ansa*-bridging can be used for the generation of highly strained, ring-tilted metallocenes, thereby offering a possibility to influence their electronic structure.[4] Ferrocenophanes have proven to be particularly valuable for an investigation of the influence of bridge length on properties such as electronic and NMR spectra, Mössbauer parameters, and metal basicity.[5−8]

Even though many *ansa*-metallocenes with a variety of bridging units are now known, those bridged by a simple hydrocarbon chain are still among the most abundant. Unfortunately, aliphatic hydrocarbon links may allow a much greater degree of flexibility than is often desirable. For example, 1,1′-disubstituted ferrocenes can on principle be fixed in chiral conformations by interannular bridges (Figure 1). However, already a propylene chain is not sufficiently rigid to prevent the molecule from racemizing.[9]

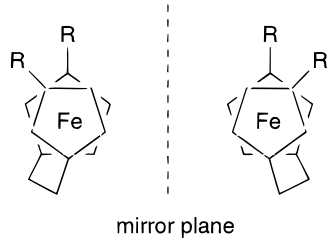

Figure 1. Schematic representation of two enantiomeric *ansa*-metallocenes. The chirality is established by an interannular bridge.

One way to minimize the conformational flexibility of metallocenes is to have aromatic moieties spanning both cyclopentadienyl rings. Examples of this class of metallocenophanes are very rare, because their synthesis is often problematic (Figure 2; **A**,[10] **B**,[11] **C**,[12] **D**[13]).

We are currently developing a novel strategy for the realization of important structural motifs in organometallic chemistry, which is based on the isoelectronic substitution of covalent carbon−carbon bonds by Lewis acid−base pairs.[14,15] In this context we have recently

† Dedicated to Professor Malcolm L. H. Green on the occasion of his 60th birthday.

‡ Telefax: (internat.) +49-89-32093473. E-mail: (internat.) wagner@zaphod.anorg.chemie.tu-muenchen.de.

⊗ Abstract published in *Advance ACS Abstracts,* March 15, 1996.

(1) Halterman, R. L. *Chem. Rev.* **1992**, *92*, 965−994.
(2) Kaminsky, W.; Külper, K.; Brintzinger, H. H.; Wild, F. R. W. P. *Angew. Chem.* **1985**, *97*, 507−508; *Angew. Chem., Int. Ed. Engl.* **1985**, *24*, 507−508.
(3) Herrmann, W. A.; Rohrmann, J.; Herdtweck, E.; Spaleck, W.; Winter, A. *Angew. Chem.* **1989**, *101*, 1536−1538; *Angew. Chem., Int. Ed. Engl.* **1989**, *28*, 1511−1512.
(4) Pudelski, J. K.; Gates, D. P.; Rulkens, R.; Lough, A. J.; Manners, I. *Angew. Chem.* **1995**, *107*, 1633−1635; *Angew. Chem., Int. Ed. Engl.* **1995**, *34*, 1506−1508.
(5) Barr, T. H.; Watts, W. E. *Tetrahedron* **1968**, *24*, 3219−3235.
(6) Barr, T. H.; Watts, W. E. *Tetrahedron* **1968**, *24*, 6111−6118.
(7) Lentzner, H. L.; Watts, W. E. *J. Chem. Soc., Chem. Commun.* **1970**, 26−27.
(8) Osborne, A. G.; Whiteley, R. H.; Meads, R. E. *J. Organomet. Chem.* **1980**, *193*, 345−357.
(9) Schlögl, K.; Peterlik, M.; Seiler, H. *Mh. Chem.* **1962**, *93*, 1309−1327.
(10) Jäkle, F.; Priermeier, T.; Wagner, M. *J. Chem. Soc., Chem. Commun.* **1995**, 1765−1766.
(11) Qian, C.; Guo, J.; Ye, C.; Sun, J.; Zheng, P. *J. Chem. Soc., Dalton Trans.* **1993**, 3441−3445.
(12) Yasufuku, K.; Aoki, K.; Yamazaki, H. *Inorg. Chem.* **1977**, *16*, 624−628.
(13) Varadarajan, A.; Johnson, S. E.; Gomez, F. A.; Chakrabarti, S.; Knobler, C. B.; Hawthorne, M. F. *J. Am. Chem. Soc.* **1992**, *114*, 9003−9011.
(14) Jäkle, F.; Mattner, M.; Priermeier, T.; Wagner, M. *J. Organomet. Chem.* **1995**, *502*, 123−130.

0276-7333/96/2315-2033$12.00/0

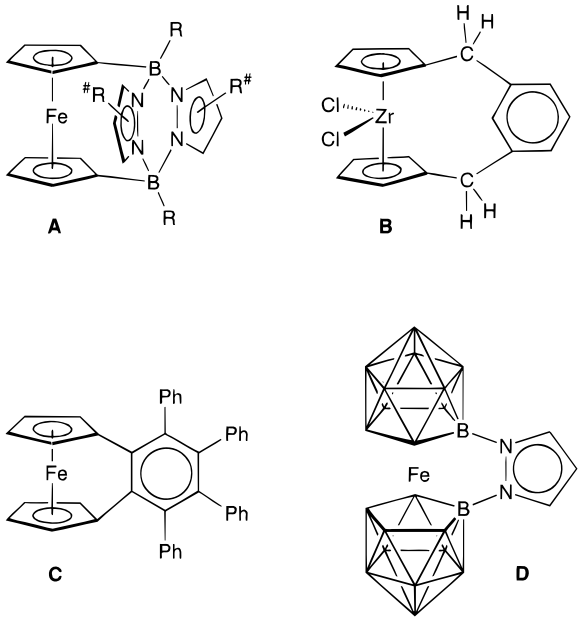

Figure 2. Structurally characterized *ansa*-metallocenes with bridges containing aromatic moieties.

reported on the facile synthesis of *ansa*-ferrocenes with *o*-phenylene type bridges, established by B−N adduct formation (**2c**; Scheme 1).[10] The purpose of this paper is to demonstrate the general applicability of our concept for the generation of a variety of ferrocenophanes **A**, to give some insight into the chemical properties of this novel class of compounds, and to investigate the factors governing bridge stability. Henceforth, individual derivatives of the general structure **A** are denoted **2a**−**i**.

From the viewpoint of synthesis, the benefit of an incorporation of *self-assembling* dative (B−N) bonds at certain positions into the molecular framework is obvious. But there are other advantages, which may be exploited for the design of ligand environments with previously unknown properties. B−N bond cleavage occurs heterolytically and reversibly, and the energy of a B−N donor−acceptor bond can be tuned over a wide range by choice of appropriate substituents at boron and nitrogen. This *reversibility* offers a chance to generate switchable interannular bridges. Depending on the temperature, solvent, or the presence of Lewis acidic or basic additives, the same metallocene could then either adopt a stereorigid *ansa*-structure or a flexible open chain conformation.

Results and Discussion

Syntheses. The key step of the synthetic pathway to compounds **2** is outlined in Scheme 1. From 1,1′-bis(dibromoboryl)ferrocene (1,1′-Fc(BBr_2)$_2$, **1a**),[16] the starting materials 1,1′-Fc($BBrCH_3$)$_2$, **1b**,[16] 1,1′-Fc(BBrOEt)$_2$, **1c**,[17] and 1,1′-Fc(BBr(NC_4H_8))$_2$, **1d**, are accessible in one step by the reaction of **1a** with 2 equiv of $Sn(CH_3)_4$, diethyl ether, or pyrrolidine/triethylamine, respectively.

The synthesis of ferrocenophane **2a** was achieved in two different ways: (1) by adding 2 equiv of pyrazole and 2 equiv of NEt_3 in toluene to a toluene solution of **1a** at −78 °C; (2) by reaction of the ethoxy-substituted ferrocenophane **2e** with 1 equiv of BBr_3. Even though the synthesis of **2a** according to method 2 requires two more steps, it is preferable to method 1, because the product is obtained in high purity and very good yield. For the preparation of all other compounds **2** it is advantageous to combine the appropriate ferrocenylborane and the required pyrazole derivative first and to add neat triethylamine afterward. **2b**−**d** and **2g,h** could readily be purified by recrystallizing the crude material from dibutyl ether. In most cases the yields are better than 70%.

Scheme 1. Synthesis of Compounds 2

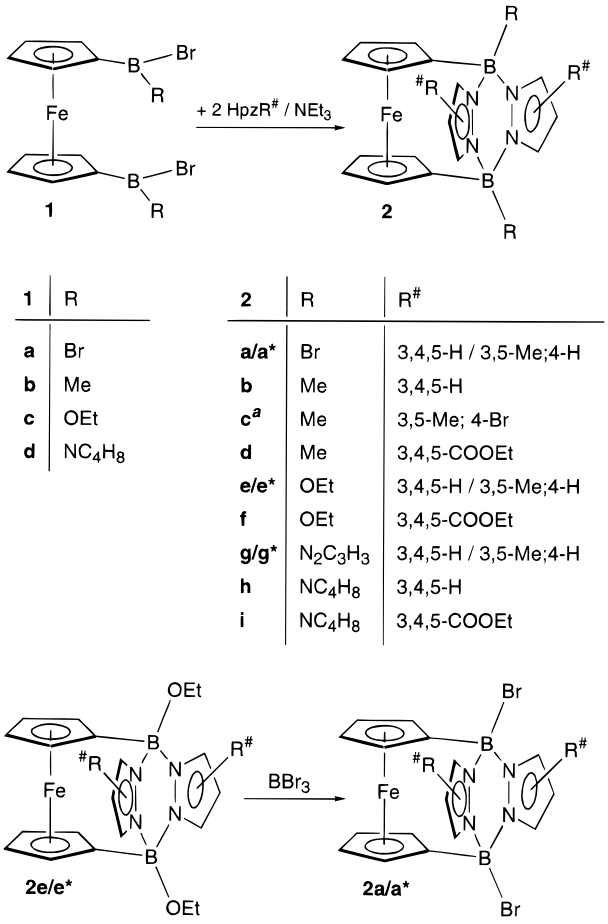

1	R
a	Br
b	Me
c	OEt
d	NC_4H_8

2	R	R#
a/a*	Br	3,4,5-H / 3,5-Me;4-H
b	Me	3,4,5-H
c[a]	Me	3,5-Me; 4-Br
d	Me	3,4,5-COOEt
e/e*	OEt	3,4,5-H / 3,5-Me;4-H
f	OEt	3,4,5-COOEt
g/g*	$N_2C_3H_3$	3,4,5-H / 3,5-Me;4-H
h	NC_4H_8	3,4,5-H
i	NC_4H_8	3,4,5-COOEt

[a] See ref 10.

Factors Favoring Intramolecular B−N Adduct Formation. We found that syntheses employing the electron-poor, sterically demanding pyrazole 3,4,5-tris(ethoxycarbonyl)pyrazole or ferrocenylboranes of lower Lewis acidity (**1c,d**) were least hampered by side reactions. For example, **2d** and **2h** do form almost quantitatively, whereas the preparation of **2b** was accompanied by a considerable amount of side product (NMR spectra of the crude materials). This side product shows the same number of signals in the ^{1}H NMR spectrum as **2b** with very similar chemical shifts. However, all resonances appear as broad humps rather

(15) Jäkle, F.; Priermeier, T.; Wagner, M. *Chem. Ber.* **1995**, *128*, 1163−1169.

(16) Ruf, W.; Renk, T.; Siebert, W. *Z. Naturforsch.* **1976**, *31b*, 1028−1034.

(17) Appel, A.; Nöth, H. Compound **1c** was published prior to us by Nöth et al. (poster presentation at the 3rd International Conference on Inorganic Chemistry, July 23−26, 1995, University of Sussex). We will therefore not describe its isolation and characterization in any detail. Only its NMR spectroscopic data are given as far as they are important for the discussion of our own results. Siebert et al. have already reported on the synthesis of 1,1′-Fc($B(OEt)_2$)$_2$ by the reaction of 1,1′-Fc(BI_2)$_2$ with diethyl ether (Renk, T.; Ruf, W.; Siebert, W. *J. Organomet. Chem.* **1976**, *120*, 1−25).

than as well-resolved, sharp signals. In the ^{11}B NMR spectrum one signal in the region of tetracoordinated boron nuclei[18] was observed, again close to the ^{11}B NMR resonance of **2b** (see below). The elemental analysis is as well close to the values calculated for **2b**. Thus, the side product probably consists of oligomeric material, where B−N donor−acceptor bonding occurred interrather than intramolecularly. However, even at temperatures as high as 200 °C, we were not able to transform any proportion of it into *ansa*-**2b**. Similar polymeric species have been obtained by Niedenzu,[19] when he transaminated the bifunctional tetrakis(dimethylamino)diborane(4) with 4 equiv of pyrazole. Our data suggest that the yield of *ansa*-**2** increases when the formation of B−N donor−acceptor bonds is slowed down (i.e. thermodynamic rather than kinetic control). Consequently, it is possible to improve the yield of *ansa*-**2b** considerably by carrying out the synthesis at higher temperature (0 °C) than in the case of the other derivatives of **2** (−78 °C).

Factors Governing the Bridge Stability. The compounds **2b**−**e,g,h** show a remarkable thermal stability and are not sensitive toward air or moisture. **2a** and **2f** are rather inert in the solid state, but their solutions tend to decompose slowly at room temperature in the presence of air. In contrast, **2i** has to be kept strictly under an inert gas atmosphere. These findings already indicate fundamentally different structures of **2a**−**h** on one hand and **2i** on the other. This conclusion is further supported by the NMR spectroscopic data of the different derivatives of **2**. The ^{11}B NMR signals of **2a**−**h** appear in the range of −1 to 7 ppm, giving good evidence for an *ansa*-ferrocene structure with pyrazabole[20] bridge and four-coordinate boron centers.[18] In contrast, the ^{11}B NMR resonance of **2i** was found at $\delta = 33.8$, which is a typical value for trivalent diaminoboranes.[18] It has to be concluded, therefore, that **2i** adopts an open chain conformation at ambient temperature. The ^{1}H and ^{13}C NMR data are in complete consonance with this interpretation. In **2a**−**h**, the hydrogen (carbon) atoms in positions 3 and 5 of the pyrazole rings give rise to only one signal. This can best be explained by the assumption of two symmetric pyrazole bridges spanning both cyclopentadienyl rings. The pyrrolidine groups in **2h** show both magnetically equivalent α-positions and β-positions at ambient temperature. This points to an unhindered rotation around the N−B bond, which excludes the pronounced N−B double bond character that could be expected in open chain-**2h**. In contrast, **2i** shows the resonances of three different ester groups and three different ^{13}C NMR signals for the pyrazole carbon atoms, which is not compatible with the highly symmetric *ansa*-ferrocene structure. Moreover, four signals for the pyrrolidine substituents in **2i** are observed as the result of N−B π bonding, which increases the barrier of B−N rotation. In the ferrocene region of the ^{1}H NMR spectrum of **2a**−**h**, a pronounced upfield shift of one of the two resonances is observed ($\delta = 3.5 \pm 0.2$). This remarkable shielding is probably due to the magnetical anisotropy of the aromatic pyrazole rings. Again, this shielding is not observed in **2i**, where the signals for the cyclopentadienyl rings appear in the usual region for 1,1′-diborylated ferrocenes.

Scheme 2. Dynamic Behavior of the Pyrazabole Bridges (E = COOEt)

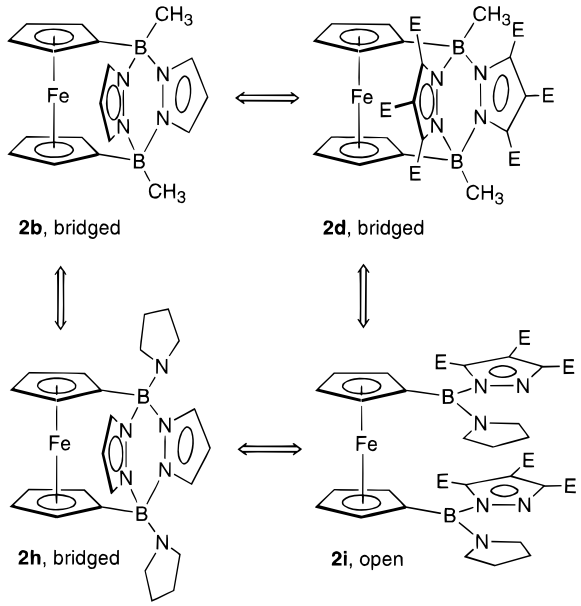

The NMR spectroscopic investigations of **2a**−**i** shed some light on the factors governing the stability of the pyrazabole bridge. Dative bonds between four-coordinate boron and pyrazole derivatives are weakened by strongly electron-withdrawing pyrazole substituents (e.g. ethoxycarbonyl), which increase the positive partial charge on the nitrogen donors. On the other hand, three-coordinate boron centers are known to be stabilized by π-donating substituents (e.g. pyrrolidine). Each of these factors on its own is too weak to prevent *ansa*-bridge formation, as indicated by the ferrocenophane structure of compounds **2d** and **2h**, which is preserved at temperatures as high as 100 °C (NMR spectroscopy; [D$_8$]toluene). However, when boron centers of low Lewis acidity are combined in the same molecule with an electron-poor pyrazole, the result is an open chain structure **2i** (NMR spectroscopic control), even at −60 °C (Scheme 2). Interestingly, no dynamic behavior of the *ansa*-bridged **2f** could be observed by high-temperature NMR spectroscopy. The π-donating ability of the oxygen atom is obviously not sufficiently high to stabilize a three-coordinate boron center in this molecule.

Nucleophilic Substitution of Br in 2a. A toluene solution of **2a** reacts slowly with pyrazole/NEt$_3$ (2 equiv) at room temperature. However, the mixture has to be kept at reflux temperature for several hours to drive the substitution of both bromides for pyrazole to completion. In the end, the pyrazolylpyrazabole **2g** is obtained in high yield (Scheme 3). On the other hand, the synthesis of **2g** from **1a** and 4 equiv of pyrazole/NEt$_3$ can be carried out even below room temperature. This means, that the formation of the pyrazabole bridge does not occur instantaneously after one pyrazole moiety has been attached to each boron atom. The attack of the third and fourth equivalent of pyrazole on open chain-**2a** is faster than the formation of *ansa*-**2a**. Nevertheless, under more drastic conditions, *ansa*-**2a** is still reactive and may serve as a useful starting material for other derivatives of **2**. This is the more surprising as

(18) Nöth, H.; Wrackmeyer, B. *Nuclear Magnetic Resonance Spectroscopy of Boron Compounds*; Springer-Verlag: Berlin, Heidelberg, New York, 1978.
(19) Brock, C. P.; Das, M. K.; Minton, R. P.; Niedenzu, K. *J. Am. Chem. Soc.* **1988**, *110*, 817−822.
(20) Trofimenko, S. *J. Am. Chem. Soc.* **1967**, *89*, 4948−4952.

Scheme 3[a]

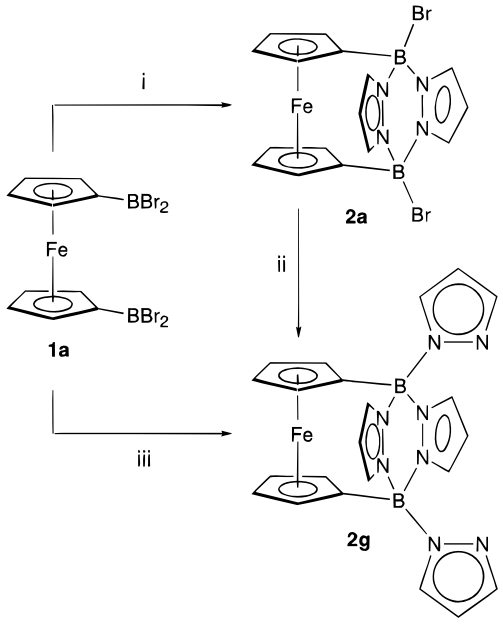

[a] Key: (i) +2 Hpz/NEt_3, toluene, −78 °C to room temperature; (ii) +2 Hpz/NEt_3, toluene reflux, 2h; (iii) +4 Hpz/NEt_3, toluene, −78 °C to room temperature.

nucleophilic substitution reactions do normally fail at bridgehead positions.[21]

We have explored some mechanistic details of the Br substitution in **2a**. A reaction of S_N2 type at *ansa*-**2a** can certainly be ruled out, because backside attack of the pyrazole molecule is prevented by the ferrocene moiety. The reaction is therefore likely to proceed either *via* open chain-**2a** (pathway 1), or *via* a kind of S_N1 mechanism with a cationic intermediate (pathway 2).

Consider pathway 1 first: The high-temperature NMR spectra (^{11}B, ^1H; [D_8]toluene; +100 °C) of **2a** did not show any significant changes compared to the room temperature ones. Thus, under the conditions of Br substitution, no NMR spectroscopically detectable concentration of open chain-**2a** is present in solution. Other evidence against an open chain intermediate stems from the reaction of **2a***, which bears methyl groups in positions 3 and 5 of the bridging pyrazole rings, with 2 equiv of pyrazole/NEt_3 (Scheme 4). After the reaction was complete (NMR spectroscopic control), insoluble material was removed by filtration. An analysis of the precipitate showed it to be exclusively triethylammonium bromide; no ferrocene containing species was found. After toluene had been removed from the filtrate *in vacuo*, the crude product was investigated by NMR spectroscopy (^{11}B, ^1H, ^{13}C). It was found to consist of the pyrazolylpyrazabole **2g*** (90%), together with a small amount (10%) of side product. The molecule **2g*** shows only one resonance for all four methyl groups and two signals for the α and *β* positions of both cyclopentadienyl rings (^1H, ^{13}C NMR spectra). This pattern fits exclusively to the highly symmetric isomer of **2g*** drawn in Scheme 4. Moreover, the only fragmentation of **2g***, which is observed in the mass spectrum (CI mode), leads to the liberation of pyrazole rather than of 3,5-dimethylpyrazole. According to the NMR spectra, the side product is definitely not another isomer of **2g*** with one

Scheme 4. Selective Synthesis of One Isomer of 2g* from 2a*: Representation of the Two Different Pathways under Consideration for a Nucleophilic Substitution at the Bridgehead Positions of 2a,a*

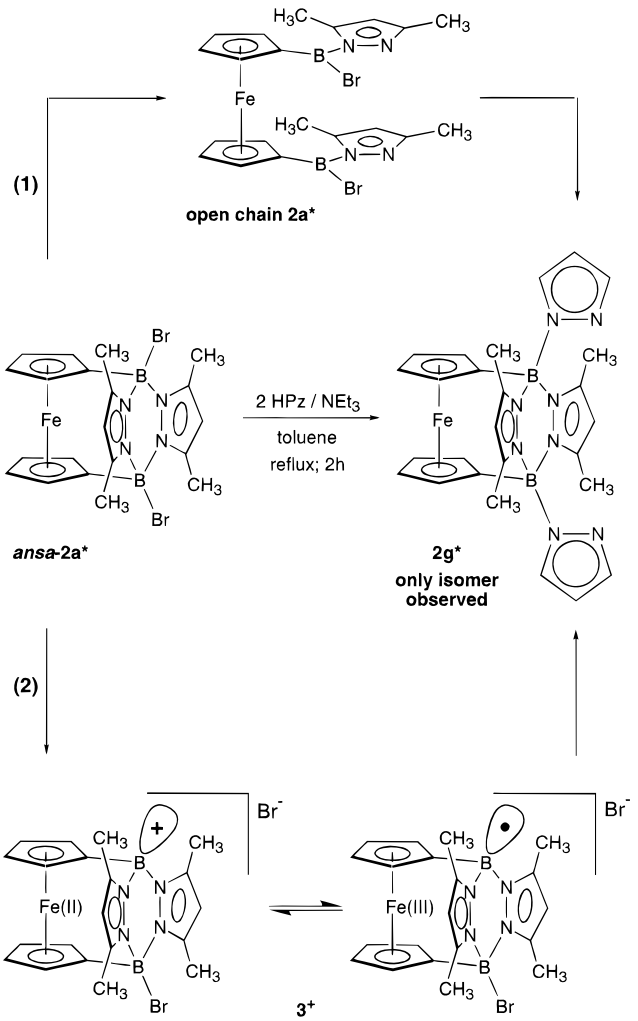

or two 3,5-dimethylpyrazolyl substituents in the *exo* positions. The crude **2g*** was again dissolved in toluene, an excess of pyrazole was added, and the mixture was kept at reflux temperature for several hours. No further reaction was observed. These findings argue against the hypothesis of an intermediate with three-coordinate boron centers, generated by cleavage of two boron−nitrogen bonds, because one would expect the positions of the different pyrazole substituents to scramble under these conditions.

Pathway 2, with its intermediate formation of $\mathbf{3}^+$, is supported by work of Niedenzu and Nöth,[22] who reported evidence for the formation of an ion pair $R_2B(\mu\text{-}pz)_2BR^+/BBr_3R^-$ in the course of the reaction of pyrazaboles with boron tribromide. However, in our case no Lewis acidic abstracting agent like BBr_3 is present, and the hypothetical cationic boron center in $\mathbf{3}^+$ would be forced into a highly unfavorable pyramidal conformation by the ferrocene unit. The latter problem could be circumvented by assuming a single-electron transfer (SET) mechanism, which is sometimes found in cases where an S_N1 mechanism seems to be indicated.[21] Such intra-ionic redox equilibria, where an electron is transferred from the iron atom to an electron-deficient

(21) March, J. *Advanced Organic Chemistry*; Wiley: New York, 1985.

(22) Niedenzu, K.; Nöth, H. *Chem. Ber.* **1983**, *116*, 1132−1153.

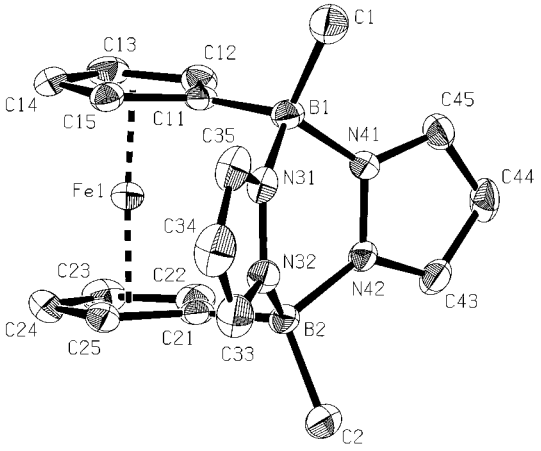

Figure 3. PLATON plot of **2b**.

ferrocene substituent and back ("redox tautomerism") are well-known in the case of ferrocenylmethylium cations.[23] Direct Fe−B interactions are present in the isoelectronic ferrocenylboranes as well,[24] and boryl radicals with electron-withdrawing substituents can be expected to have a pyramidal shape, similar to the analogous carbon-centered specimen.[25] Therefore, this intramolecular SET mechanism, though entirely speculative, certainly merits consideration and further experimental studies on this subject are in progress in our laboratory.

Molecular Structure

2b crystallizes from toluene/hexane as yellow platelets in the space group $P\bar{1}$ with two crystallographically independent molecules in the asymmetric unit (**2b**−**A**, **2b**−**B**). Since both molecules possess very similar structures, only one of them (**2b**−**A**) is shown (Figure 3). The complete set of structure data for **2b**−**A** and **2b**−**B** is available on request.[26]

2b can be viewed both as a ferrocenophane and as a pyrazabole[20] bridged with a ferrocene moiety. Only few neutral bridged pyrazaboles RB(μ-pz)$_2$(μ-E)BR (pz = pyrazolyl; E = −S_2−,[27] **4**, −Se−,[28] **5**, −Se_2−,[28] **6**, −OBEtO−,[29] **7**), have been synthesized and structurally characterized so far. Of all those, **2b** possesses by far the largest bridging unit ($C_{11}\cdots C_{21}$ = 3.19 Å), followed by **6** and **7** (**6**, Se−Se = 2.4 Å; **7**, O···O = 2.4 Å).

From a series of crystal structures of unbridged pyrazabole derivatives, the central B_2N_4 moiety is known to adopt planar, chair, and boat conformations, depending on both the boron and the pyrazole substituents.[22] Furthermore, a theoretical investigation of the related 9,10-dihydroanthracene showed the potential energy surface of this compound to be very shallow with respect to conformational changes of the central unit.[30,31] The boat conformation of the B_2N_4 ring, which is imposed by the bridge in **2b** and **4**−**7**, is therefore unlikely to cause any significant strain in the molecule. Consequently, in ferrocenophane **2b**, the cyclopentadienyl rings are still almost parallel with a tilt angle of only 3.8°. These findings suggest that the pyrazabole moiety is able to adapt very well to the steric requirements of the ferrocene core. The folding angles between the BN_2 planes and the N_4 plane of the pyrazabole unit are 30.3 and 31.5°, and the two pyrazole rings form a roof angle of 37.5°. Since a shorter bridge enhances the boat conformation of the B_2N_4 ring, the roof angle in **6** is 46.6°, and in **5** an even higher value of 74° was found.

The B−N bond lengths in **2b** (1.573(4)−1.589(4) Å) are similar to those of the other bridged pyrazaboles with O−BR−O and Se−Se bridges (Table 3) but about 0.02 Å longer than those in pyrazaboles **4** and **5** with their short −S_2− and −Se− bridges. The N−N bonds, as well as all bond angles, lie within the normally observed ranges.

The X-ray structure data reveal no significant changes in the geometry of the pyrazabole fragment of our *ansa*-ferrocene, compared to free pyrazaboles. It is therefore understandable why the well-known chemical stability of pyrazaboles is preserved in the bridging unit of **2b**.

Table 1. Summary of Crystallographic Data for Complex 2b

compd	**2b**
formula	$C_{18}H_{20}B_2FeN_4$
fw	369.9
cryst dimens, mm	0.3 × 0.2 × 0.2
cryst syst	triclinic
space group	$P\bar{1}$
temp, K	193 K
a, Å	8.948(2)
b, Å	13.750(3)
c, Å	15.294(4)
α, deg	112.40(1)
β, deg	92.09(2)
γ, deg	95.64(2)
V, Å^3	1776(1)
D_{calc}, g·cm^{-3}	1.424
Z	4
radiation (λ, Å)	Mo K_α (0.710 73)
no. of tot. reflns	6335
no. of obsd reflns	4692
no. of params	612
μ, cm^{-1}	8.8
final *R*	0.0410
final R_w	0.0248

Conclusion

We have demonstrated that B−N donor−acceptor bonds can be exploited for the facile synthesis of complex structural motifs, which would be much harder to realize by conventional organic chemistry. The final step occurs via *self-association* of diborylated ferrocenes, 1,1′-Fc(BBrR)$_2$, and various derivatives of pyrazole, HpzR‡, upon simple mixing of both components. This type of preparation allows variations of the electronic properties of boron and the pyrazole moieties separately from each other and over a wide range. The stability of the molecular framework of the *ansa*-ferrocenes **2a**−**h** is as high as could be expected for the all-carbon analogs.

(23) Ashkenazi, P.; Cais, M. *Angew. Chem.* **1972**, *84*, 1106−1107; *Angew. Chem., Int. Ed. Engl.* **1972**, *11*, 1027−1028.
(24) Appel, A.; Jäkle, F.; Priermeier, T.; Schmid, R.; Wagner, M. *Organometallics* **1996**, *15*, 1188−1194.
(25) Pauling, L. *J. Chem. Phys.* **1969**, *51*, 2767−2769.
(26) Further details of the crystal structure investigation are available on request from the Fachinformationszentrum Karlsruhe, Gesellschaft für wissenschaftlich-technische Information mbH, D-76344 Eggenstein-Leopoldshafen, Germany, on quoting the depository number CSD 404942, the names of the authors, and the literature citation.
(27) Das, M. K.; Niedenzu, K.; Nöth, H. *Inorg. Chem.* **1988**, *27*, 1112−1114.
(28) Yalpani, M.; Boese, R.; Köster, R. *Chem. Ber.* **1990**, *123*, 713−718.
(29) Hsu, L.-Y.; Mariategui, J. F.; Niedenzu, K.; Shore, S. G. *Inorg. Chem.* **1987**, *26*, 143−147.
(30) Lipkowitz, K. B.; Rabideau, P. W.; Raber, D. J.; Hardee, L. E.; Schleyer, P. v. R.; Kos, A. J.; Kahn, R. A. *J. Org. Chem.* **1982**, *47*, 1002−1005.
(31) Rabideau, P. W. *Acc. Chem. Res.* **1978**, *11*, 141−147.

Table 2. Atomic Coordinates ($\times 10^4$) and Isotropic Thermal Parameters ($Å^2 \times 10^4$) with Esd's in Parentheses for the Non-Hydrogen Atoms of Compound 2b

atom	*x*	*y*	*z*	*U*(eq)[a]
		Compound **2b**-A		
Fe(1)	0.25692(5)	0.13052(4)	0.48156(3)	0.0215
B(1)	0.1036(4)	0.3250(3)	0.6318(2)	0.0237
B(2)	0.0864(3)	0.2997(3)	0.4248(2)	0.0248
C(1)	0.0717(5)	0.3833(3)	0.7400(2)	0.0386
C(2)	0.0358(4)	0.3332(4)	0.3391(3)	0.0377
C(11)	0.1925(3)	0.2242(2)	0.6105(2)	0.0213
C(12)	0.1305(3)	0.1169(2)	0.5851(2)	0.0265
C(13)	0.2471(4)	0.0510(3)	0.5706(2)	0.0306
C(14)	0.3857(4)	0.1180(3)	0.5887(2)	0.0281
C(15)	0.3520(3)	0.2229(3)	0.6137(2)	0.0241
C(21)	0.1752(3)	0.1988(2)	0.3941(2)	0.0225
C(22)	0.1124(4)	0.0907(3)	0.3639(2)	0.0296
C(23)	0.2292(4)	0.0248(3)	0.3439(2)	0.0330
C(24)	0.3680(4)	0.0909(3)	0.3616(2)	0.0336
C(25)	0.3342(3)	0.1960(3)	0.3907(2)	0.0261
N(31)	0.1938(3)	0.4073(2)	0.5970(2)	0.0245
N(32)	0.1824(3)	0.3970(2)	0.5047(2)	0.0239
C(33)	0.2773(4)	0.4753(3)	0.3983(3)	0.0354
C(34)	0.3501(4)	0.5348(3)	0.5854(3)	0.0427
C(35)	0.2955(3)	0.4909(2)	0.6463(2)	0.0328
N(41)	−0.0498(2)	0.2932(2)	0.5681(2)	0.0226
N(42)	−0.0581(2)	0.2799(2)	0.4753(2)	0.0222
C(43)	−0.2019(3)	0.2488(3)	0.4410(2)	0.0286
C(44)	−0.2280(4)	0.2405(3)	0.5103(2)	0.0322
C(45)	−0.1893(3)	0.2698(3)	0.5890(2)	0.0292
		Compound **2b**-B		
Fe(2)	0.29611(5)	0.38945(4)	0.8772(3)	0.0265
B(3)	0.5562(4)	0.2396(3)	0.0855(2)	0.0274
B(4)	0.3021(4)	0.1513(3)	−0.0723(2)	0.0294
C(3)	0.7072(4)	0.2347(3)	0.1423(3)	0.0407
C(4)	0.2167(5)	0.0630(3)	−0.1669(3)	0.0460
C(51)	0.4891(3)	0.3490(2)	0.1323(2)	0.0240
C(52)	0.5192(3)	0.4423(2)	0.1121(2)	0.0307
C(53)	0.4362(4)	0.5221(3)	0.1698(2)	0.0381
C(54)	0.3539(4)	0.4804(3)	0.2276(2)	0.0345
C(55)	0.3865(3)	0.3766(3)	0.2054(2)	0.0275
C(61)	0.2218(3)	0.2563(2)	−0.0298(2)	0.0278
C(62)	0.2432(4)	0.3477(3)	−0.0530(2)	0.0357
C(63)	0.1522(4)	0.4237(3)	−0.0002(3)	0.0422
C(64)	0.0710(4)	0.3823(3)	0.0581(3)	0.0399
C(65)	0.1123(3)	0.2793(3)	0.0386(2)	0.0336
N(71)	0.5837(3)	0.2189(2)	−0.0206(2)	0.0257
N(72)	0.4701(3)	0.1806(2)	−0.0908(2)	0.0254
C(73)	0.5267(4)	0.1820(3)	−0.1708(2)	0.0368
C(74)	0.6763(4)	0.2218(3)	−0.1518(3)	0.0409
C(75)	0.7081(4)	0.2436(3)	−0.0578(2)	0.0346
N(81)	0.4340(3)	0.1455(2)	0.0777(2)	0.0290
N(82)	0.3213(3)	0.1054(2)	0.0072(2)	0.0284
C(83)	0.2280(4)	0.0341(3)	0.0261(3)	0.0417
C(84)	0.2799(5)	0.0295(3)	0.1093(3)	0.0518
C(85)	0.4100(5)	0.0981(3)	0.1394(2)	0.0422

[a] Equivalent isotropic *U* is defined as one-third of the trace of the orthogonalized $\mathbf{U}_{ij}$ tensor.

Table 3. Selected Bond Distances (Å) and Angles (deg) and Dihedral Angles (deg) of Compound 2b-A

B(1)−C(1)	1.590(4)	B(2)−C(2)	1.611(4)
B(1)−C(11)	1.598(4)	B(2)−C(21)	1.589(4)
B(1)−N(31)	1.589(4)	B(2)−N(32)	1.573(4)
B(1)−N(41)	1.576(4)	B(2)−N(42)	1.582(4)
N(31)−N(32)	1.363(3)	N(41)−N(42)	1.359(3)
C(1)−B(1)−C(11)	114.6(3)	C(2)−B(2)−C(21)	114.5(3)
C(1)−B(1)−N(31)	109.5(3)	C(2)−B(2)−N(32)	109.3(3)
C(1)−B(1)−N(41)	109.3(3)	C(2)−B(2)−N(42)	108.9(2)
C(11)−B(1)−N(31)	109.5(2)	C(21)−B(2)−N(32)	110.4(2)
C(11)−B(1)−N(41)	110.4(2)	C(21)−B(2)−N(42)	109.9(2)
N(31)−B(1)−N(41)	103.0(2)	N(32)−B(2)−N(42)	103.3(2)
C(11)−C(15)‖ C(21)−C(25)	3.8	N(31)−C(35)‖ N(41)−C(45)	37.5
B(1)N(31)N(41)‖ N(31)N(32)N(41)N(42)	30.3	B(2)N(32)N(42)‖ N(31)N(32)N(41)N(42)	31.5
B(1)N(31)N(32)B(2)‖ B(1)N(41)N(42)B(2)	44.3		

The *reversibility* of dative B−N pairing (i.e. the possibility to break and re-form these bonds repeatedly) is yet another advantage of donor−acceptor links compared to covalent carbon−carbon bonds. Tuning of the substitution pattern of boron and pyrazole makes it possible to influence the stability of the pyrazabole bridges and hence the conformational rigidity of the ferrocenophane. For example, **2b** preserves its *ansa*-structure at temperatures higher than 100 °C, whereas **2i** adopts an unbridged, open-chain conformation even at −60 °C.

We are currently exploring the potential of compounds **2** for the generation of novel ligand environments. One approach is to fix additional donor groups at the bridgehead boron centers and thereby to place transition metal atoms inside the pocket generated by both pyrazole units. Another topic of further research will be the question whether similar pyrazabole *ansa*-bridges can be introduced into other metallocenes (e.g. zirconocene).

Experimental Section

General Considerations. All reactions and manipulations of air-sensitive compounds were carried out in dry, oxygen-free argon using standard Schlenkware or in an argon-filled drybox. Solvents were freshly distilled under N_2 from Na/K alloy−benzophenone (toluene, hexane, Et_2O, *n*-Bu_2O) or from CaH_2 (CH_2Cl_2) prior to use. IR: solvent toluene or CH_2Cl_2 (organic and organometallic compounds), Perkin-Elmer 1650 FTIR. NMR: Jeol JMN-GX 400 and Bruker DPX 400 (abbreviations: s = singlet, d = doublet, tr = triplet, vtr = virtual triplet, br = broad). ^{11}B NMR spectra were referenced to external $BF_3 \cdot Et_2O$. MS (CI, FAB mode): Finnigan MAT 90. Elemental analyses: Microanalytical laboratory of the Technische Universität München.

The compounds **1a**,[16] **1b**,[16] and **1c**[17] were synthesized according to literature procedures.

Synthesis of 1c. A solution of 0.92 g (1.75 mmol) of 1,1′-Fc(BBr_2)$_2$ in 40 mL of toluene was reacted with neat diethyl ether (0.27 g, 3.64 mmol) at room temperature. After 5 d the formation of **1c** was completed (^{11}B NMR spectrum). All volatiles were removed in vacuo, and the resulting **1c** was used without further purification.

^{11}B NMR (128.3 MHz, $CDCl_3$): δ 37.8 ($h_{1/2}$ = 270 Hz). ^{1}H NMR (400.0 MHz, $CDCl_3$): δ 1.41 (t, 6H, J(HH) = 7.3 Hz, OCH_2CH_3), 4.36 (q, 4H, J(HH) = 7.3 Hz, OCH_2CH_3), 4.50 (s, 8H, C_5H_4). ^{13}C NMR (100.5 MHz, $CDCl_3$): δ 16.9 (OCH_2CH_3), 65.6 (OCH_2CH_3), 74.4 (C_5H_4), 75.6 (C_5H_4), n.o. (C_5H_4-*ipso*).

Synthesis of 1d. To a mixture of pyrrolidine (0.30 g, 4.22 mmol) and NEt_3 (0.43 g, 4.25 mmol) in 40 mL of toluene, a solution of 1,1′-Fc(BBr_2)$_2$ (1.11 g, 2.11 mmol) in 40 mL of toluene was added dropwise with stirring at −78 °C. The reaction mixture was slowly warmed to room temperature and stirred for 12 h. After filtration through a fine-porosity frit, the filtrate was evaporated to dryness; **1d** was used without further purification.

^{11}B NMR (128.3 MHz, $CDCl_3$): δ 34.4 ($h_{1/2}$ = 300 Hz). ^{1}H NMR (400.0 MHz, $CDCl_3$): δ 1.86 (mult, 4H, NCH_2CH_2), 1.96 (mult, 4H, NCH_2CH_2), 3.49 (t, 4H, J(HH) = 6.7 Hz, NCH_2CH_2), 3.63 (t, 4H, J(HH) = 6.7 Hz, NCH_2CH_2), 4.44 (vtr, 4H, J(HH) = 1.8 Hz, C_5H_4), 4.50 (vtr, 4H, J(HH) = 1.8 Hz, C_5H_4). ^{13}C NMR (100.5 MHz, $CDCl_3$): δ 25.6 (NCH_2CH_2), 27.4 (NCH_2CH_2), 49.9 (NCH_2CH), 52.8 (NCH_2CH_2), 73.2 (C_5H_4), 76.6 (C_5H_4), n.o. (C_5H_4-*ipso*). CI-MS: *m*/*z* 504 [(M^+); 100%], 425 [(M^+ − Br); 23%].

Synthesis of 2a. Method 1. To a solution of 1,1′-Fc(BBr_2)$_2$ (0.85 g, 1.62 mmol) in 35 mL of toluene, a mixture of pyrazole

(0.22 g, 3.23 mmol) and NEt_3 (0.33 g, 3.26 mmol) in 20 mL of toluene was added dropwise with stirring at −30 °C. The resulting slurry was slowly warmed to room temperature and then kept at reflux temperature for 3 h. It was cooled to room temperature and filtered through a fine-porosity frit, and all volatiles were removed from the filtrate in vacuo. A pale yellow solid was obtained, which was recrystallized from CH_2Cl_2/hexane (1:2) to give yellow crystals of **2a** (0.27 g, 33%).

Method 2. To a solution of 0.88 g (2.05 mmol) of **2e** in 20 mL of toluene, a toluene solution (15 mL) of 0.51 g (2.05 mmol) of BBr_3 was added with stirring at −40 °C. The mixture was slowly warmed to room temperature and stirred for 5 h. All volatiles were evaporated *in vacuo*, and the yellow solid residue was recrystallized from a mixture of CH_2Cl_2/hexane (2:1). Yield: 0.85 g, 83%.

^{11}B NMR (128.3 MHz, $CDCl_3$): δ 1.2 ($h_{1/2}$ = 250 Hz). ^{1}H NMR (400.0 MHz, $CDCl_3$): δ 3.45 (vtr, 4H, J(HH) = 1.8 Hz, C_5H_4), 4.12 (vtr, 4H, J(HH) = 1.8 Hz, C_5H_4), 6.67 (t, 2H, J(HH) = 2.3 Hz, pz-H4), 8.51 (d, 4H, J(HH) = 2.3 Hz, pz-H3,5). ^{13}C NMR (100.5 MHz, $CDCl_3$): δ 70.3 (C_5H_4), 71.1 (C_5H_4), n.o. (C_5H_4-*ipso*), 106.4 (pz-C4), 138.9 (pz-C3,5). CI-MS: *m*/*z* 498 [(M^+); 100%], 419 [(M^+ − Br); 30%]. Anal. Calcd for $C_{16}H_{14}B_2Br_2FeN_4$: C, 38.47; H, 2.80; N, 11.21. Found: C, 38.47; H, 3.10; N, 11.17.

Synthesis of 2a*. Starting from **2e*** (1.22 g, 2.51 mmol) and BBr_3 (0.63 g, 2.51 mmol), the synthesis of **2a*** was achieved similar to **2a** (method 2). Yield: 1.21 g, 87%.

^{11}B NMR (128.3 MHz, $CDCl_3$): δ 1.0 ($h_{1/2}$ = 250 Hz). ^{1}H NMR (400.0 MHz, $CDCl_3$): δ 2.82 (s, 12H, pz-CH_3), 3.61 (br, 4H, C_5H_4), 4.34 (br, 4H, C_5H_4), 6.12 (s, 2H, pz-H4). ^{13}C NMR (100.5 MHz, $CDCl_3$): δ 18.6 (pz-CH_3), 71.9 (C_5H_4), 74.2 (C_5H_4), n.o. (C_5H_4-*ipso*), 113.4 (pz-C4), 149.4 (pz-C3,5). CI-MS: *m*/*z* 554 [(M^+)]. Anal. Calcd for $C_{20}H_{22}B_2Br_2FeN_4$: C, 43.23; H, 3.99; N, 10.08; Br, 28.76. Found: C, 43.24; H, 4.02; N, 10.48; Br, 28.76.

Synthesis of 2b. A solution of 1,1′-Fc($BBrCH_3$)$_2$ (0.97 g, 2.45 mmol) in 20 mL of toluene was added dropwise with stirring to a solution of pyrazole (0.34 g, 5.00 mmol) in 20 mL of toluene at 0 °C. To the resulting yellow suspension neat NEt_3 (0.50 g, 4.94 mmol) was added, and the mixture was slowly warmed to room temperature and stirred for 12 h. After filtration through a fine-porosity frit, volatile material was removed from the filtrate in vacuo to yield a pale yellow microcrystalline solid. The crude product was redissolved in toluene/pentane (1:2) and filtered again from insoluble material. The solution was kept at −25 °C for 12 h to give yellow crystals (0.75 g, 83%) of **2b**.

^{11}B NMR (128.3 MHz, $CDCl_3$): δ −0.4 ($h_{1/2}$ = 200 Hz). ^{1}H NMR (400.0 MHz, $CDCl_3$): δ 0.63 (s, 6H, BCH_3), 3.28 (vtr, 4H, J(HH) = 1.5 Hz, C_5H_4), 3.99 (vtr, 4H, J(HH) = 1.5 Hz, C_5H_4), 6.51 (t, 2H, J(HH) = 2.3 Hz, pz-H4), 7.86 (d, 4H, J(HH) = 2.3 Hz, pz-H3,5). ^{13}C NMR (100.5 MHz, $CDCl_3$): δ 7.4 (br, BCH_3), 69.6 (C_5H_4), 70.1 (C_5H_4), 83.7 (br, C_5H_4-*ipso*), 105.2 (pz-C4), 133.9 (pz-C3,5). CI-MS: *m*/*z* 370 [(M^+); 100%], 355 [(M^+ − CH_3); 8%]. Anal. Calcd for $C_{18}H_{20}B_2FeN_4$: C, 58.46; H, 5.45; N, 15.15. Found: C, 58.19; H, 5.43; N, 15.36.

Synthesis of 2d. A solution of 1.02 g (3.59 mmol) of Hpz-(3,4,5-COOEt) in 30 mL of toluene was treated at −78 °C with a toluene solution of 1,1′-Fc($BBrCH_3$)$_2$ (0.71 g, 1.80 mmol). After addition of neat NEt_3 (0.38 g, 3.76 mmol) the mixture was warmed to room temperature, stirred for 12 h, and filtered through a fine-porosity frit. All volatile compounds were removed from the filtrate in vacuo, and the resulting yellow solid was recrystallized from boiling di-*n*-butyl ether to give yellow needles of **2d**. Yield: 1.27 g (88%).

IR (CH_2Cl_2): ν(CO) 1727 s, 1749 vs cm^{-1}. ^{11}B NMR (128.3 MHz, $CDCl_3$) δ 4.0 ($h_{1/2}$ = 1200 Hz). ^{1}H NMR (400.0 MHz, $CDCl_3$): δ 0.56 (s, 6H, BCH_3), 1.36 (t, 6H, J(HH) = 7.3 Hz, $COOCH_2CH_3$), 1.41 (t, 12H, J(HH) = 7.3 Hz, $COOCH_2CH_3$), 3.66 (br, 4H, C_5H_4), 4.05 (br, 4H, C_5H_4), 4.30−4.50 (mult, 12H, $COOCH_2CH_3$). ^{13}C NMR (100.5 MHz, $CDCl_3$): δ 8.5 (br, BCH_3), 13.7 ($COOCH_2CH_3$), 14.0 ($COOCH_2CH_3$), 61.7 ($COOCH_2CH_3$), 63.3 ($COOCH_2CH_3$), 69.5 (C_5H_4), 69.9 (C_5H_4), 79.1 (br, C_5H_4-*ipso*), 112.2 (pz-C4), 143.2 (pz-C3,5), 159.5 (CO), 160.6 (CO). FAB-MS: *m*/*z* 802 [(M^+); 100%]. Anal. Calcd for $C_{36}H_{44}B_2FeN_4O_{12}$: C, 53.90; H, 5.52; N, 6.98. Found: C, 54.05; H, 5.81; N, 6.99.

Synthesis of 2e. To a solution of **1c** (0.80 g, 1.75 mmol) in 40 mL of toluene, a solution of pyrazole (0.24 g, 3.53 mmol) in 30 mL of toluene was added at −78 °C with stirring. The mixture was then treated with neat NEt_3 (0.35 g, 3.46 mmol) and allowed to warm to room temperature. After filtration and evaporation of all volatiles in vacuo, the yellow oily residue was redissolved in 20 mL of hexane. A small amount of insoluble material was filtered off, hexane was removed from the filtrate in vacuo, and **2e** was obtained as an orange oil. Yield: 0.56 g (74%).

^{11}B NMR (128.3 MHz, $CDCl_3$): δ 4.1 ($h_{1/2}$ = 170 Hz). ^{1}H NMR (400.0 MHz, $CDCl_3$): δ 1.30 (t, 6H, J(HH) = 6.7 Hz, OCH_2CH_3), 3.44 (s, 4H, C_5H_4), 3.71 (q, 4H, J(HH) = 6.7 Hz, OCH_2CH_3), 4.09 (s, 4H, C_5H_4), 6.52 (t, 2H, J(HH) = 1.4 Hz, pz-H4), 7.98 (d, 4H, J(HH) = 1.4 Hz, pz-H3,5). ^{13}C NMR (100.5 MHz, $CDCl_3$): δ 18.4 (OCH_2CH_3), 60.5 (OCH_2CH_3), 69.7 (C_5H_4), 71.4 (C_5H_4), n.o. (C_5H_4-*ipso*), 105.2 (pz-C4), 133.8 (pz-C3,5). Because of the oily nature of **2e**, a proper elemental analysis could not be obtained. However, a comparison of the NMR data of **2e** and **2e*** can be taken as a proof for its chemical constitution.

Synthesis of 2e*. **2e*** was obtained from 1.77 g (3.88 mmol) of **1c** and 0.75 g (7.76 mmol) of 3,5-dimethylpyrazole similar to **2e** as a yellow solid. Yield: 1.49 g (79%).

^{11}B NMR (128.3 MHz, $CDCl_3$): δ 4.0 ($h_{1/2}$ = 400 Hz). Due to rotational hindrance, many of the ^{1}H and ^{13}C NMR resonances are broad at room temperature; therefore, the spectra at +90 °C are given. ^{1}H NMR (400.0 MHz, [D_8]toluene, +90 °C): δ 1.07 (t, 6H, J(HH) = 6.7 Hz, OCH_2CH_3), 2.36 (s, 12H, pz-CH_3) 3.30 (mult, 4H, 4H, C_5H_4, OCH_2CH_3), 3.97 (vtr, 4H, J(HH) = 1.8 Hz, C_5H_4), 5.54 (s, 2H, pz-H4). ^{13}C NMR (100.5 MHz, [D_8]toluene, +90 °C): δ 16.6 (pz-CH_3), 21.0 (OCH_2CH_3), 62.9 (OCH_2CH_3), 73.7 (C_5H_4), 75.0 (C_5H_4), n.o. (C_5H_4-*ipso*), 112.8 (pz-C4), 149.7 (pz-C3,5). CI-MS: *m*/*z* 486 [(M^+); 100%], 441 [(M^+ − OEt); 16%]. Anal. Calcd for $C_{24}H_{32}B_2FeN_4O_2$·0.5(toluene): C, 62.07; H, 6.82; N, 10.53. Found: C, 61.86; H, 6.78; N, 10.54.

Synthesis of 2f. To a toluene solution of **1c** (0.60 g, 1.31 mmol), a toluene solution of Hpz(3,4,5-COOEt) (0.74 g, 2.60 mmol) was added dropwise with stirring at −78 °C. Neat NEt_3 (0.26 g, 2.60 mmol) was added, and the mixture was warmed to room temperature and stirred for 12 h. Insoluble material was removed by filtration, the filtrate was evaporated to dryness, and the crude product was washed twice with 5 mL of diethyl ether. It was recrystallized from toluene/hexane to give 0.78 g (69%) of **2f**.

IR (CH_2Cl_2): ν(CO) 1726 s, 1747 vs cm^{-1}. ^{11}B NMR (128.3 MHz, $CDCl_3$): δ 6.6 ($h_{1/2}$ = 500 Hz). ^{1}H NMR (400.0 MHz, $CDCl_3$): δ 0.99 (t, 6H, J(HH) = 7.0 Hz, OCH_2CH_3), 1.31 (t, 6H, J(HH) = 7.0 Hz, $COOCH_2CH_3$), 1.35 (t, 12H, J(HH) = 7.0 Hz, $COOCH_2CH_3$), 3.27 (q, 4H, J(HH) = 7.0 Hz, OCH_2CH_3), 3.77 (vtr, 4H, J(HH) = 1.7 Hz, C_5H_4), 4.11 (vtr, 4H, J(HH) = 1.7 Hz, C_5H_4), 4.24 (q, 4H, J(HH) = 7.0 Hz, $COOCH_2CH_3$), 4.30 (mult, 8H, $COOCH_2CH_3$). ^{13}C NMR (100.5 MHz, $CDCl_3$): δ 13.7 ($COOCH_2CH_3$), 14.1 ($COOCH_2CH_3$), 16.2 (OCH_2CH_3), 61.2, 61.4 (OCH_2CH_3, $COOCH_2CH_3$), 62.8 ($COOCH_2CH_3$), 70.5 (C_5H_4), 71.3 (C_5H_4), n.o. (C_5H_4-*ipso*), 111.5 (pz-C4), 142.4 (pz-C3,5), 159.5 (CO), 159.8 (CO). Anal. Calcd for $C_{38}H_{48}B_2FeN_4O_{14}$: C, 52.94; H, 5.61; N, 6.50. Found: C, 53.17; H, 5.81; N, 6.51.

Synthesis of 2g. Pyrazole (0.45 g, 6.67 mmol) was dissolved in 60 mL of toluene, cooled to −78 °C, and treated with a solution of 1,1′-Fc(BBr_2)$_2$ (0.88 g, 1.67 mmol) in 20 mL of toluene. After 5 min, neat NEt_3 (0.70 g, 6.90 mmol) was added, and the mixture was warmed to room temperature and stirred for 12 h. Insoluble material was removed by filtration, and the solvent was removed from the filtrate under reduced

pressure. The crude product was recrystallized from boiling di-*n*-butyl ether to give yellow needles of **2g**. Yield: 0.60 g (76%).

^{11}B NMR (128.3 MHz, $CDCl_3$): δ 1.3 ($h_{1/2}$ = 170 Hz). ^{1}H NMR (400.0 MHz, $CDCl_3$): δ 3.58 (vtr, 4H, J(HH) = 1.8 Hz, C_5H_4), 4.24 (vtr, 4H, J(HH) = 1.8 Hz, C_5H_4), 6.31 (vtr, 2H, J(HH) = 1.8 Hz, *exo*-pz-H4), 6.43 (t, 2H, J(HH) = 2.3 Hz, μ-pz-H4), 7.27 (d, 4H, J(HH) = 2.3 Hz, μ-pz-H3,5), 7.66 (d, 2H, J(HH) = 1.8 Hz, *exo*-pz-H3), 7.78 (d, 2H, J(HH) = 1.8 Hz, *exo*-pz-H5). ^{13}C NMR (100.5 MHz, $CDCl_3$): δ 70.9 (C_5H_4), 71.7 (C_5H_4), n.o. (C_5H_4-*ipso*), 105.0 (pz-C4), 106.1 (pz-C4), 135.6 (μ-pz-C3,5), 136.7 (br, *exo*-pz-C3), 142.9 (*exo*-pz-C5). CI-MS: *m*/*z* 474 [(M^+); 100%], 407 [($M^+ - N_2C_3H_3$); 60%]. Anal. Calcd for $C_{22}H_{20}B_2FeN_8$: C, 55.76; H, 4.25; N, 23.64. Found: C, 55.69; H, 4.24; N, 23.54.

Synthesis of 2g*. Pyrazole (0.05 g, 0.72 mmol) and NEt_3 (0.07 g, 0.72 mmol) were dissolved in 20 mL of toluene at room temperature. **2a*** (0.20 g, 0.36 mmol) was dissolved in 15 mL of toluene at +50 °C. The warm solution was added dropwise with stirring to the solution of the amines, and the reaction mixture was kept at reflux temperature for 2 h. Insoluble material (0.14 g; 100% $HNEt_3Br$ = 0.13 g) was removed by filtration, and toluene was evaporated from the filtrate in vacuo. The yellow solid residue was analyzed without further purification. Yield: 0.18 g (94%).

^{11}B NMR (128.3 MHz, $CDCl_3$): δ 0.8 ($h_{1/2}$ = 150 Hz). ^{1}H NMR (400.0 MHz, $CDCl_3$): δ 1.49 (s, 12H, pz-CH_3), 3.52 (vtr, 4H, J(HH) = 1.8 Hz, C_5H_4), 4.19 (vtr, 4H, J(HH) = 1.8 Hz, C_5H_4), 5.92 (s, 2H, μ-pz-H4), 6.23 (vtr, 2H, J(HH) = 1.8 Hz, *exo*-pz-H4), 7.48 (d, 2H, J(HH) = 1.8 Hz, *exo*-pz-H3), 7.75 (d, 2H, J(HH) = 1.8 Hz, *exo*-pz-H5). ^{13}C NMR (100.5 MHz, $CDCl_3$): δ 10.5 (pz-CH_3), 70.7 (C_5H_4), 71.1 (C_5H_4), n.o. (C_5H_4-*ipso*), 105.5 (*exo*-pz-C4), 110.5 (μ-pz-C4), 137.0 (*exo*-pz-C3), 142.6 (*exo*-pz-C5), 147.0 (μ-pz-C3,5). CI-MS: *m*/*z* 530 [(M^+); 100%], 463 [($M^+ - N_2C_3H_3$); 60%]. Anal. Calcd for $C_{26}H_{28}B_2FeN_8$: C, 58.92; H, 5.32; N, 21.14. Found (crude product): C, 57.69; H, 5.47; N, 19.92 (absence of bromine confirmed).

Synthesis of 2h. A solution of **1d** (1.06 g, 2.10 mmol) in 50 mL of toluene was reacted at −78 °C with a toluene solution of pyrazole (0.28 g, 4.11 mmol). Subsequently, neat NEt_3 (0.43 g, 4.25 mmol) was added, and the reaction mixture was warmed to room temperature and stirred for 12 h. After filtration and evaporation of the solvent in vacuo, the crude product was recrystallized from hexane. Yield: 0.92 g (91%).

^{11}B NMR (128.3 MHz, $CDCl_3$): δ 2.0 ($h_{1/2}$ = 220 Hz). ^{1}H NMR (400.0 MHz, $CDCl_3$): δ 1.79 (mult, 8H, NCH_2CH_2), 2.92 (mult, 8H, NCH_2CH_2), 3.30 (br, 4H, C_5H_4), 4.00 (br, 4H, C_5H_4), 6.43 (br, 2H, pz-H4), 7.79 (br, 4H, pz-H3,5). ^{13}C NMR (100.5 MHz, $CDCl_3$): δ 27.0 (NCH_2CH_2), 48.1 (br, NCH_2CH_2), 68.8 (C_5H_4), 70.8 (C_5H_4), n.o. (C_5H_4-*ipso*), 104.4 (pz-C4), 134.2 (pz-C3,5). CI-MS: *m*/*z* 480 [(M^+); 100%], 410 [($M^+ - NC_4H_8$); 8%]. Anal. Calcd for $C_{24}H_{30}B_2FeN_6$: C, 60.05; H, 6.30; N, 17.51. Found: C, 59.67; H, 6.19; N, 17.17.

Synthesis of 2i. A solution of **1d** (1.07 g, 2.12 mmol) in 20 mL of toluene was reacted with a toluene (20 mL) solution of Hpz(3,4,5-COOEt) (1.20 g, 4.22 mmol) at −78 °C. Neat NEt_3 (0.43 g, 4.25 mmol) was added, and the mixture was warmed to room temperature and stirred for 12 h. Insoluble material was removed by filtration, the solvent was evaporated from the filtrate in vacuo, and a red oily residue was obtained. The oil solidified upon treatment with 20 mL of hexane. The hexane was removed with a filter cannula, and the crude product was dissolved in toluene/hexane. Orange crystals of **2i** were obtained from this solution at −25 °C. Yield: 1.22 g (63%).

IR (CH_2Cl_2): ν(CO) 1716 s, 1730 s cm^{-1}. ^{11}B NMR (128.3 MHz, $CDCl_3$, RT): δ 33.8 ($h_{1/2}$ = 1200 Hz). ^{1}H NMR (400.0 MHz, [D_8]toluene, 100 °C; the room temperature spectrum is complicated due to rotational hindrance. Therefore, the spectrum at 100 °C is given): δ 0.85 (t, 6H, J(HH) = 7.3 Hz, $COOCH_2CH_3$), 1.07 (t, 6H, J(HH) = 7.3 Hz, $COOCH_2CH_3$), 1.19 (t, 6H, J(HH) = 7.3 Hz, $COOCH_2CH_3$), 1.32 (mult, 4H, NCH_2CH_2), 1.55 (mult, 4H, NCH_2CH_2), 2.84 (br, 4H, NCH_2CH_2), 3.41 (br, 4H, NCH_2CH_2), 3.86 (q, 4H, J(HH) = 7.3 Hz, $COOCH_2CH_3$), 4.14 (q, 4H, J(HH) = 7.3 Hz, $COOCH_2CH_3$), 4.0−4.2 (very br, 4H, C_5H_4), 4.29 (q, 4H, J(HH) = 7.3 Hz, $COOCH_2CH_3$), 4.39 (br, 4H, C_5H_4). ^{13}C NMR (100.5 MHz, $CDCl_3$, RT): δ 13.8, 14.1, 14.2 ($COOCH_2CH_3$), 25.5, 26.7 (NCH_2CH_2), 48.4, 48.7 (NCH_2CH_2), 61.2, 61.6, 61.8 ($COOCH_2CH_3$), 67.4 (br), 72.9, 73.3, 74.3, 74.7 (C_5H_4), 120.3 (pz-C4), 135.6 (br, pz-C3,5), 142.9 (pz-C3,5), 158.5, 161.2, 164.0 (CO). FAB-MS: *m*/*z* 912 [(M^+); 100%], 629 [($M^+ - N_2C_3(COOEt)_3$); 10%]. Anal. Calcd for $C_{42}H_{54}B_2FeN_6O_{12}$: C, 55.29; H, 5.97; N, 9.21. Found: C, 55.26; H, 6.26; N, 9.13.

Crystal Structure Determination of 2b.[26] A yellow crystal of **2b** was selected in a perfluorinated oil and mounted in a glass capillary on an automatic four-circle diffractometer (CAD4, Enraf Nonius). Final lattice parameters were obtained by least-squares refinement of 25 high-angle reflections (graphite monochromator, λ = 0.710 73 Å, Mo $K_{\bar{\alpha}}$). Data: $C_{18}H_{20}B_2FeN_4$, M = 369.9, triclinic system, space group $P\bar{1}$ (No. 2) with two crystallographically independent molecules in the asymmetric unit, a = 8.948(2) Å, b = 13.750(3) Å, c = 15.294(4) Å, α = 112.40(1)°, β = 92.09(2)°, γ = 95.64(2)°, V = 1776(1) Å^3, crystal size 0.3 × 0.2 × 0.2 mm, D_{calc} = 1.424 g cm^{-3}, Z = 4. Data were collected at 192(±1) K, using the ω-scan method, with maximal acquisition time 90 s for a single reflection. Data were corrected for Lorentz and polarization terms; an absorption correction was applied on the base of azimuthal reflections (T = 0.92−1.0). The extinction parameter[32] was determined to be 14.389, with 6335 data measured, 5116 independent reflections, 1013 with negative intensity, and 4692 reflections with $I > 1.0\sigma(I)$ used for refinement. The structure was solved by the Patterson method[33] and refined with standard difference Fourier techniques.[34] All hydrogen atoms were located in difference Fourier maps and refined isotropically. A total of 612 parameters were refined, with 7.7 data per parameter, weighting scheme $w = 1/\sigma_{F_o}^2$, shift/error < 0.0001 in the last cycle of refinement, residual electron density +0.30 e Å^{-3}, 0.73 Å near C21, and −0.42 e Å^{-3}, R = 0.041, R_w = 0.025, and minimized function $\sum w(|F_o| - |F_c|)^2$.

Acknowledgment. We are grateful to Prof. Dr. W. A. Herrmann (Technical University of Munich) for his generous support. Financial funding by the "Bayerischer Forschungsverbund Katalyse" (FORKAT) and by the "Fonds der Chemischen Industrie" is acknowledged.

Supporting Information Available: Tables of complete positional and thermal parameters and bond distances and angles (8 pages). Ordering information is given on any current masthead page.

OM9509305

(32) Equation (22): Larson, A. C. *Crystallographic Computing*; Munksgaard: Copenhagen, 1969.

(33) Sheldrick, G. M. SHELXS-86, Universität Göttingen, Germany, 1986.

(34) Watkin, D. J.; Betteridge, P. W.; Carruthers, J. R. CRYSTALS; Oxford, England, 1986.